Boundary layer stabilization via physical and thermodynamic roughness

Francis Lacombe and Jean-Pierre Hickey ●

Mechanical and Mechatronics Engineering, University of Waterloo,
200 University Avenue W., N2L 3G1, Ontario, Canada

The coupling effect of physical and thermodynamic wall roughness is investigated using nonlinear parabolized stability equations. A patch of five sinusoidal physical and wall temperature variations, denoted here as roughness, is positioned upstream of the typical transition location of a zero-pressure gradient flat-plate boundary layer at $M = 0.7$. Using only thermodynamic roughness on a flat plate, we note the stabilizing effect of cooling strips, whereas, the heating has a destabilizing effect on the stability of Tollmien-Schlichting waves. The combined effect of physical roughness patch superimposed on the thermodynamic roughness results in a synergetic coupling effect that delays the transition. The addition of sinusoidally varying wall temperature to physical roughness can stabilize the boundary layer through a spectral narrowing of the instability modes and the generation of off-peak frequencies. Thus, the physical roughness with cooling results in a more stable boundary layer compared to cooling alone, a finding that could help improve temperature-based active laminar flow control devices.

I. INTRODUCTION

Drag reduction in aerospace is one of the main drivers of technological innovation. By delaying the transition to turbulence, thus, increasing the laminar footprint over the body, a favorable reduction of frictional forces can be obtained, resulting in improved operational efficiencies. Although it is desirable to delay the transition to turbulence, it remains technically difficult to achieve a robust, resilient, and energy-efficient approach to stabilize the boundary layer. Various physical mechanisms can be used to delay transition. Natural laminar flow (NLF) design has shown the potential to deliver significant drag reduction. By considering the pressure distribution on the wetted surface during the design stage, engineers can adjust the favorable pressure gradients in specific regions to stabilize the boundary layer, thus, naturally delaying the transition. NLF design considerations have been applied to airfoil shape optimization in a number of works [1,2]. Although the stabilization potential is acknowledged, cross-flow-driven instabilities, which dominate the swept wings or nacelle transition, often limit the efficacy of stabilizing effects [3].

Although more complex than NLF, laminar flow control (LFC) is another paradigm to delay transition, which seeks to increase the resilience of the boundary layer to transitional instabilities through active or passive means. Active flow controls have also shown a very significant potential to delay the boundary transition through the use of synthetic jets and plasma actuation (e.g., Ref. [4]). Similarly, boundary layer suction targets inflectional instabilities in the base flow, although it has been shown to be most effective in low-Mach number regimes [5]. Other works by Fransson and Alfredsson [6] showed that cross-flow wall blowing can, unexpectedly, be both stabilizing and destabilizing depending on the parameters. The slow adoption of active laminar flow control approaches by industry is attributed to the relative mechanical complexity of the systems and the often unfavorable integrated energy balance. In this regard, *passive* laminar flow control approaches remain particularly attractive. Bioinspired leading edge design [7] or riblets [8] have been used as

passive flow control mechanisms that target the modification of energetic turbulent structures in the boundary layer. These approaches tend to have a small operational window, which can result in an increase in drag outside the target range. On the transitional side, Zahn and Rist [9] highlighted that surface imperfections, such as a deep gap, could result in a standing acoustic wave that can be tuned to dampen TS modes in transitional flows. Fransson *et al.* [10] showed that well-designed cylindrical roughness elements can thwart the growth of the most unstable waves in a boundary layer through the generation of streaks, which originate from the hairpin structures [11,12]. This idea was later extended to study miniature vortex generators [13], but these vortical flow generators can lead to subcritical transition with deleterious effects on drag. A more recent paradigm for delaying the transition combines both NLF and LFC. The premise is to complement the pressure gradient-based design with a laminar flow control approach; this combined approach, known as hybrid laminar flow control, has been used for several decades [14] with sustained promise.

Boundary layer control through localized heating or cooling represents one of the classical approaches to active flow control. As localized heating or cooling only slightly modifies the local density and viscosity, it imparts a modest modification to the boundary layer compared to more aggressive flow control technologies, such as blowing or suction. Additionally, localized heating can represent an energy neutral active flow control approach through reuse of engine waste heat on the nacelle, for example. The use of thermodynamic flow control has been proposed in both laminar and turbulent flows. In a fully turbulent channel flow, for example, targeted heating can be used to modulate coherent structures and reduce drag [15,16]. In the transitional regime, a series of investigations have been carried out for nearly half a century. As a general rule, uniform cooling has a stabilizing effect on laminar boundary layers. The wall cooling tends to create a more stable and resilient velocity profile, analogous to the effect of a favorable pressure gradient in a boundary layer [17]. Inversely, uniform heating plays a destabilizing role. Although heating a gas increases its local viscosity, thus, reducing the local Reynolds number, it can result in a local inflectional instability of the velocity profile, which leads to a precocious transition to turbulence.

Unlike uniform heating, strategically placed strips of localized heating, denoted here as *thermodynamic roughness*, can help delay the transition. Dogval *et al.* [18] experimentally showed that localized heating delays transition in two-dimensional and three-dimensional boundary layers, but if the transition mechanism is due to cross-flow instabilities, the heating remains ineffective. Physically, although localized heating is destabilizing, if the strips are placed slightly upstream of the transition point, the downstream, the unheated wall effectively becomes a *cooled wall*. The unheated wall acts to restabilize the boundary layer and delays the overall transition to turbulence [19]. Localized heating strips have been suggested as an active flow control approach for supersonic transport [20]. Heating strips can also be used to stabilize the first mode in supersonic flows [21]. The stabilizing effect was nuanced by Ref. [22] who suggested that the heating strip only had a stabilizing effect if the temperature of the "cooled" wall remained below the adiabatic wall temperature. Several recent contributions have continued to optimize these flow stabilization strategies [23–27].

Adding physical roughness to heated or cooled walls greatly impacts the stability of the boundary layer. Localized cooling increases the density of the near-wall fluid, and the boundary layer becomes more sensitive to roughness as it artificially increases the apparent height of the incoming obstacles [28]. It also modifies the growth rate near or in separated flow regions [28,29]. The combination of physical and thermodynamic roughness represents a laminar flow control strategy that combines both passive (physical roughness) and active (thermodynamic roughness) approaches. The modal response of these physical and thermodynamic wall roughnesses on the compressible Blasius flow remains unclear. To this end, we first conduct a nonlinear parabolized stability equations (PSE) parametric study on localized wall heating/cooling under high subsonic conditions. Then, the focus is turned toward a comparative study of the coupling effect between the use of physical and thermodynamic roughness. The potential benefits of distributed temperature strips and smooth physical roughness are explored and contrasted with the transitional characteristics of a flat-plate boundary layer.

II. METHODOLOGY

A. Numerical tools

The stability of a zero-pressure gradient flat-plate boundary layer with nonuniform wall temperature and small-scale sinusoidal wall roughness is investigated using the nonlinear PSE. The PSEs are a subset of the modal stability theory which can be used to investigate weakly nonparallel flows, such as spatially evolving laminar boundary layers. Modal stability based approaches decompose the flow quantities into a steady $\overline{q}$ and fluctuating component, the latter being defined in PSE as

$$q' = \hat{q}(x, y) \exp\left(-i \int_x \alpha_n dx - \omega t\right). \tag{1}$$

The compressible Navier-Stokes equations are then linearized and rewritten in terms of fluctuating variables, which are then replaced by the above modal description to obtain

$$\left\{ \mathcal{L}\hat{q} + \mathcal{L}_x \frac{\partial \hat{q}}{\partial x} + \mathcal{L}_y \frac{\partial \hat{q}}{\partial y} + \mathcal{L}_{yy} \frac{\partial^2 \hat{q}}{\partial y^2} \right\}_n = \left\{ \exp\left(-i \int_x \alpha_n dx\right) \mathcal{F}'' \right\}_n, \tag{2}$$

where the matrices $\mathcal{L}$, $\mathcal{L}_y$, $\mathcal{L}_{yy}$, and $\mathcal{L}_x$ only depend on the base flow, the streamwise wave-number (α), and temporal wave-number (ω). The system of Eqs. (2) must be solved sequentially for each mode, hence, the subscript n. The coupling between modes occurs through the term $\mathcal{F}''$, which contains the nonlinear forcing terms.

In the present paper, we use KRYPTON, an open source PSE code that can be used to compute both the base and the fluctuating flow computations of the compressible Navier-Stokes equations in a curvilinear coordinate system [30]. Here, we assess the stability of the flow using the nonlinear stability calculations of this solver. In classical PSE theory, each mode is represented discretely, i.e., by a dominant mode and its subharmonics. Here, we use a novel approach, developed by Kuehl *et al.* [31] in which each mode is represented using a finite-bandwidth approach. The method is analogous to a wave-packet approach, except that each mode is represented continuously; this allows for a better energy redistribution among the modes, which helps to study spectral broadening processes [31]. The nonlinear interactions are evaluated numerically, in the physical space, and projected in the frequency domain using an efficient *fast Fourier-transformed* algorithm. Details of the code are provided in Ref. [30] and are not repeated for brevity.

The Reynolds and Mach reference numbers are defined on the basis of the *inlet* state and are defined as

$$\text{Re}_\delta = \frac{u_\infty \delta}{\nu_\infty} = \sqrt{\frac{u_\infty x_0}{\nu_\infty}}, \quad Ma = \frac{u_\infty}{\sqrt{\gamma R T_\infty}}, \tag{3}$$

where the subscript ∞ represents the reference values of the freestream, subscript 0 represents the inlet conditions, and $\delta = \sqrt{\frac{\nu_\infty x_0}{u_\infty}}$ is a length scale proportional to the thickness of the boundary layer at x_0 (where $\delta_{99} \approx 5\delta$).

B. Setup

Previous work by Lacombe and Hickey [32] and Lacombe [33] favorably compared the predictive nature of nonlinear PSE and with direct numerical simulations (DNSs) and showed that the results are nearly indistinguishable when the surface roughness remains small. The main discrepancies between the two approaches arise when nonlinear interactions cause a modification to the base flow. As thermodynamic heating provides a very subtle change to the main flow characteristics, and the computational cost is about four orders of magnitude lower than the equivalent DNS, the present paper focuses solely on the use of nonlinear PSE to parametrically investigate the stability characteristics of this flow.

Here, we focus on the effect of a patch of two-dimensional sinusoidal roughness of a flat-plate boundary layer at a freestream Mach number of about 0.7. We distinguish between *physical*
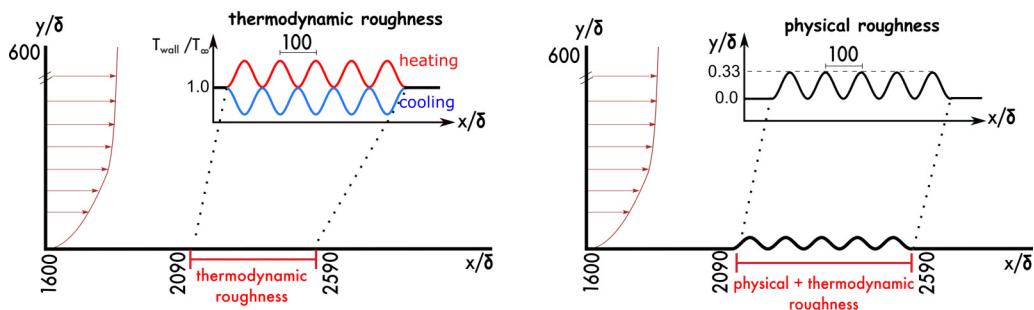
FIG. 1. Numerical setups for the thermodynamic roughness (left) and the combination of physical and thermodynamic roughness (right). The figure is not to scale.

roughness, which is a sinusoidally varying wall height, and *thermodynamic roughness*, which is sinusoidally varying wall temperature (cooled or heated). This will be referred to as cooling/heating strips. The setup, very similar to the physical roughness investigated in Ref. [32] using direct numerical simulations, consists of a canonical spatially evolving zero-pressure gradient, flat-plate boundary layer with a patch of either thermodynamic roughness (Sec. III A) or a combination of thermodynamic and physical roughness (Sec. III B). Figure 1 shows the numerical setup with the relevant characteristic dimensions for both cases. The height of the roughness of the baseline cases is $h = 0.33\delta$—corresponding to about 6% of the inlet boundary layer height. The roughness (both physical and thermodynamic) elements are located between $x/\delta = [2090, 2590]$, and the wavelength of the roughness is $x/\delta = 100$. The position and characteristics of the roughness patch were carefully selected to ensure that the transition to turbulence occurs downstream of the roughness patch, while maintaining the validity of the PSE approximation through the comparison of the same setup with DNS [33]. As the roughness induces a premature transition without immediately tripping the flow, it allows us to isolate the transition from the wall roughness. This facilitates the comparison between physical smooth roughness and thermodynamic roughness.

For all the cases investigated in this paper, the laminar base flow is first computed using the compressible Navier-Stokes solver in KRYPTON (each case has a unique laminar base flow solution), which is based on the same numerical methods as the PSE solver. We then inject a superimposed low-amplitude perturbation at the inlet of the domain. The perturbation is represented by uniformly distributed modes from $F = 0$ to $F = 72$, that is, $F \in [0, 6, 12, \ldots, 72]$. As shown in Fig. 2, the frequency content of the perturbations consists of a dominant mode centered at $F = 18$ [Tollmien-Schlichting, or (TS)] with a bandwidth $\sigma_F = 4.5$ and its subharmonic mode, centered at $2F$, with
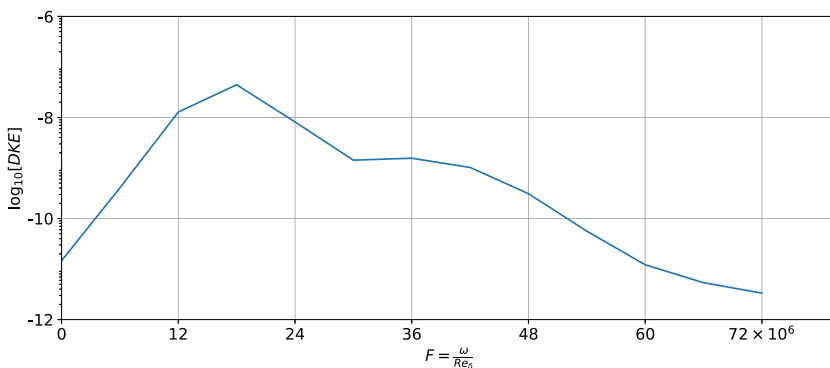

FIG. 2. Perturbation frequency content characterized by the disturbance kinetic energy (DKE) at the inlet.
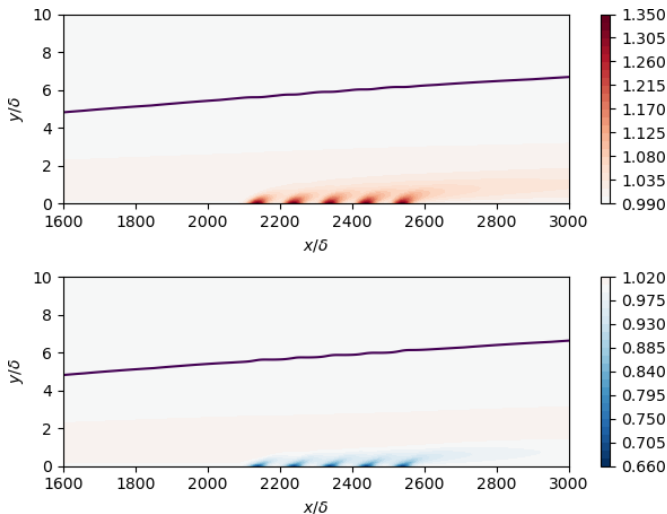
FIG. 3. Contour plot of the temperature for the case with heating strips (top) and cooling strips (bottom). The solid line is the boundary layer thickness ($\delta_{0.99}$).

a bandwidth of $\sigma_{2F} = \sqrt{2}\sigma_F$, or equivalently $\sigma_\omega = 0.0072$ and $\sigma_{2\omega} = 0.01018$. The methodology used to determine σ_F and σ_{2F}, is detailed in Ref. [32]. The TS mode is determined on the basis of the linear stability analysis of the baseline case at $x/\delta = 3000$. Since the amplitude of the mode depends on the wall normal direction, the intensity of the fluctuation at the inlet is based on the maximum amplitude of the perturbation and is scaled by the freestream velocity. In practice, in the PSE theory, the only variable on which it is possible to impose a nontrivial condition is the fluctuating pressure at the wall. Therefore, in practice, the boundary condition is applied to the variable $\hat{p}$. We must then iterate on the value of $\hat{p}(0)$ until the maximum velocity fluctuation, which is computed from the whole frequency spectrum, reaches the desired value, in this case 0.18% of the freestream velocity at the inlet.

III. RESULTS

A. Effect of thermodynamic roughness alone

First, we consider the case of a sinusoidal wall temperature variation on a flat-plate boundary layer (Fig. 1, left). A parametric study of the different wall temperature effects are investigated. The wavelength of the wall temperature roughness remains identical, but we vary the amplitude of the temperature from $T_{\text{wall}}/T_\infty = 0.665$ (cooling) to $T_{\text{wall}}/T_\infty = 1.335$ (heating). The flat part of the wall (up- and downstream of roughness) is maintained at an isothermal temperature of $T_{\text{wall}}/T_\infty = 1$.

Figure 3 shows the temperature contour of the two limit heating and cooling cases. Although the presence of heating or cooling strips has a very limited impact on the thickness of the boundary layer (see comparative boundary layer thickness in Fig. 3), the effect is most noticeable on the friction coefficient of the wall shown in Fig. 4 where the laminar and mean flow distortion (MFD) skin-friction coefficients are shown. These estimates can be used to determine the approximate transition location. Adding cooling strips stabilizes the boundary layer, whereas, adding heating strips drastically destabilizes the flow. This result was expected because the location of the wall temperature inhomogeneity is in the modal growth region [18]. Although it is possible to qualitatively estimate the location of the transition based on wall friction in Fig. 4, it is more convenient to define a quantitative criterion to better highlight any physical trends that we could observe. Here, we define the beginning of transition based on the MFD wall friction, transition
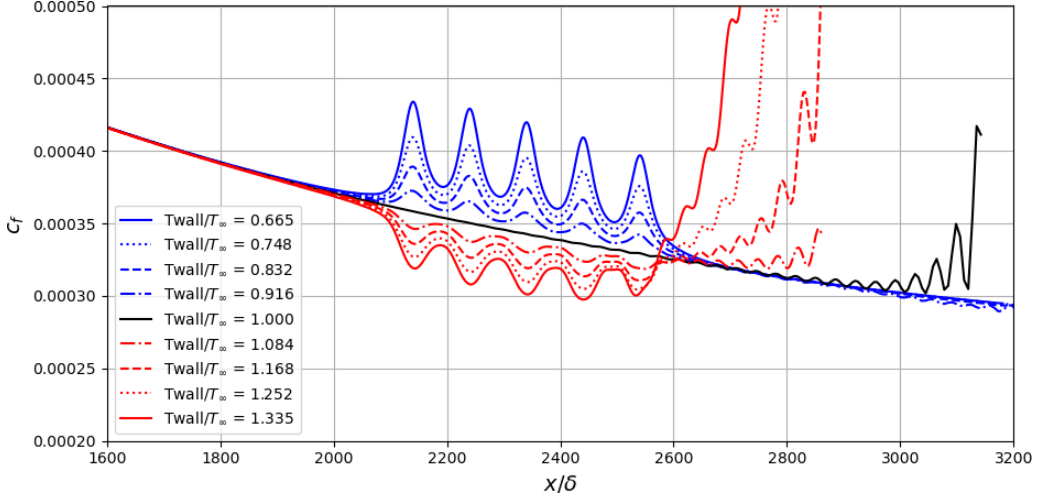
FIG. 4. Effect of cooling and heating (without physical roughness) on the friction coefficient along the stream direction. The coefficient of friction is computed based on the sum of the laminar and MFD contributions.

to turbulence is triggered once the absolute of the MFD wall friction exceeds 5% of the laminar friction, that is, when $|\frac{\partial \hat{u}_{(0,0)}}{\partial y} / \frac{\partial u_{\text{lam}}}{\partial y}| > 0.05$. Figure 5 shows the relative transitional Reynolds number as a function of the wall temperature amplitude; $\Delta \text{Re}_{\text{tr}}$ is defined as the difference between the transition Reynolds number with and without thermodynamic roughness. Interestingly, heating precipitates the transition and the variation of the transition location (defined through $\Delta \text{Re}_{\text{tr}}$) follows an exponential function with the magnitude of the wall temperature. Cooling has a strong stabilizing effect as previously seen in Fig. 4. We note a clear plateau around $\Delta \text{Re}_{\text{tr}} \approx 50$ in Fig. 5, which implies that we can reach a non-negligible delay in transition with a minimal wall temperature variation. After the plateau, with sufficient cooling, we regain an exponential type of transition delay with temperature. This dual mode of stabilization with cooling strips is attributed to the different mechanisms of boundary stabilization. If the wall temperature variation is small ($T_{\text{wall}}/T_{\infty} = [0.8, 0.99]$), the cooling primarily dampens the TS instability modes, which
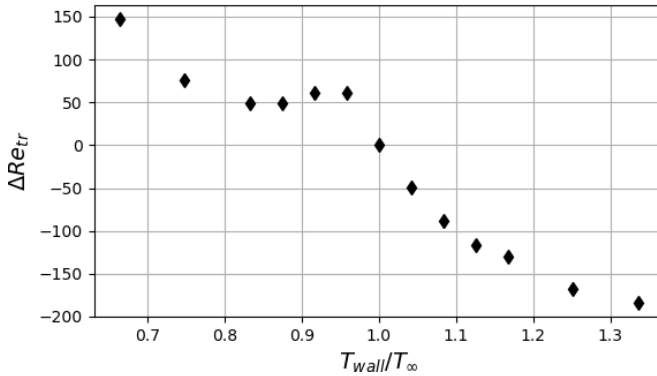

FIG. 5. Effect of cooling and heating on the transition location (obtained using the nonlinear parabolized stability equations NPSEs). The zero-pressure gradient (ZPG) flat plate at $M = 0.7$. The transition criteria is met when $|\frac{\partial \hat{u}_{(0,0)}}{\partial y} / \frac{\partial u_{\text{lam}}}{\partial y}| > 0.05$.
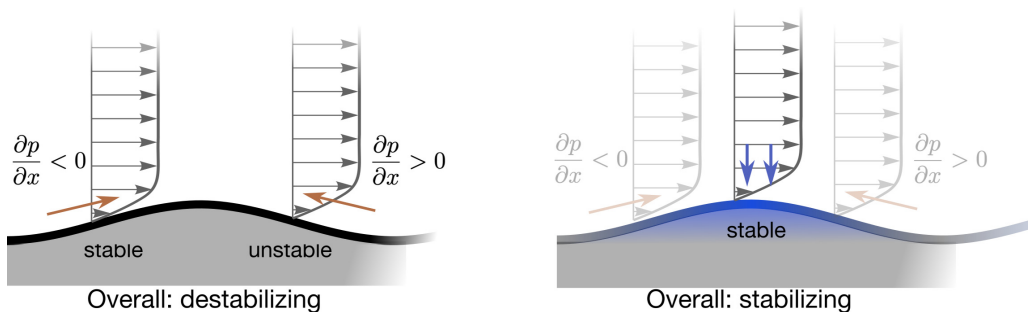
FIG. 6. The smooth physical roughness (without cooling, left) is a sequence of destabilizing and stabilizing pressure gradients. Localized cooling at the peaks (right) where the flow is labile, stabilizes the sequence.

are present in the boundary layer—the mode damping leads to a plateau in the transition delay. At higher wall cooling [$(T_{\text{wall}}/T_\infty < 0.8)$], the stabilization arises through a modification of the base flow through the increase in density near the wall, making the base flow more resilient to instabilities.

B. Combined effect of thermodynamic and physical roughness

In laminar boundary layers, wall cooling has a stabilizing effect on the flow by increasing the near wall density and damping TS modes, thus, making the flow more resilient to transition. In this regard, it was reported that the stabilizing effect of cooling strips is similar to that of a smooth forward-facing step (FFS) [29], whereas, a backward-facing step (BFS) is analogous to wall heating, thus, destabilizing. However, this conclusion is only valid for a smooth geometry as the impact of discrete FFS and BFS is always destabilizing and increases with step height [34]. Following this logic, a sinusoidal smooth wall roughness can be understood as a sequence of smooth FFS followed by a smooth BFS. Therefore, the sinusoidally varying physical roughness can be loosely interpreted as analogous to sinusoidally varying thermodynamic roughness. Since the effect of BFS is generally *more* destabilizing in comparison to the stabilizing effect of a FFS, a sequence of multiple humps is, therefore, considered destabilizing. Now, let us consider the superposition of sinusoidally varying thermodynamic roughness that is in phase with the most unstable points of the physical roughness, i.e., at the crest of each physical roughness hump. We now have a different sequence in which a favorable pressure gradient enhances the stability (as the flow goes up the physical roughness), followed by a maximum thermodynamic roughness, which has a stabilizing effect when cooled (destabilizing effects when heated), and finally the descent into the through which destabilizes the base flow. The proposed mechanism is illustrated in Fig. 6. In this context, it is not clear whether the overall effect will be stabilizing or destabilizing. The quantification of this effect is investigated in this section. The physical setup of the combination of physical and thermodynamic roughness is shown in Fig. 1, right.

Figure 7 shows the temperature contour of two extreme heating (top) and cooling (bottom) cases in phase with the physical roughness; we note a very similar boundary layer height modification over the physical roughness. Figure 8 (left) shows the evolution of the DKE along the stream-wise direction. The red, blue, and black curves correspond, respectively, to the $T_{\text{wall}}/T_\infty = 1.335$, $T_{\text{wall}}/T_\infty = 0.665$, and isothermal cases. The solid line represents the combination of physical ($h = 0.33\delta$) and thermodynamic roughness, whereas, the dashed line corresponds to the cases with only thermodynamic roughness (similar to the previous subsection). We see that the physical roughness has a slightly destabilizing effect in the isothermal and heated cases. Interestingly, the presence of physical roughness (humps) and thermodynamic cooling tends to enhance the effect of the cooling strips alone, resulting in an enhanced stabilization of the boundary layer. The cooling strips stabilize the flow by acting on three fronts: (1) they dampen the instability modes in the flow;
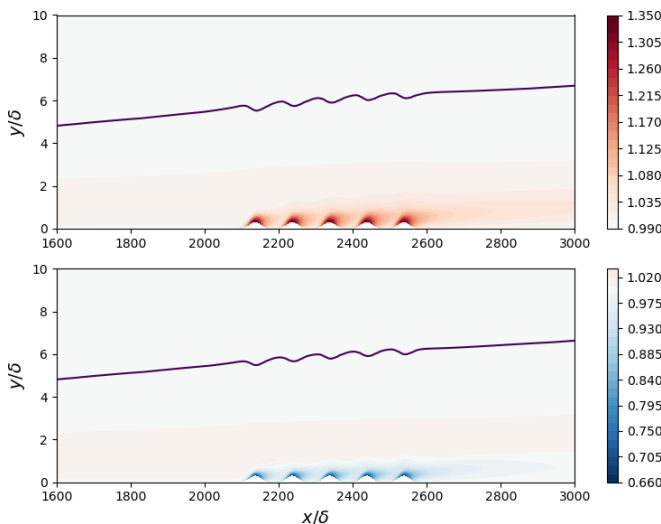
FIG. 7. Contour plot of the temperature for the case with heating strips (top) and cooling stips (bottom). Both cases feature a sequence of five sinusoidal humps of $h = 0.33\delta$. The solid line is the boundary layer thickness ($\delta_{0.99}$).

(2) they reduce the inflectional instability by locally decreasing the viscosity (thereby modifying the velocity profile); (3) they induce a downward velocity by increasing the local density, which partly cancels the effect of the flow going down the valley. These combined effects act to enhance the resilience of the boundary layers to instabilities. In Fig. 8 (right), the effect of the phase between the cooling strips and the roughness humps on the growth of the disturbance is investigated. The simulations until now considered the thermal and physical roughnesses to be perfectly in phase (maximum cooling at the crests), which corresponds to the stabilization mechanism described earlier. Here, we consider the perfectly out-of-phase case in which the maximum cooling is in the trough, the purple curve corresponds to the *out-of-phase* case. When the cooling is not in phase with the physical roughness, the flow is destabilized compared to the cooling alone. This finding supports the stabilization mechanism presented in Fig. 6. The effect of the physical roughness height is considered in Fig. 9. We consider a cooled wall case at $T_{\text{wall}}/T_{\infty} = 0.912$ (located in the plateau of
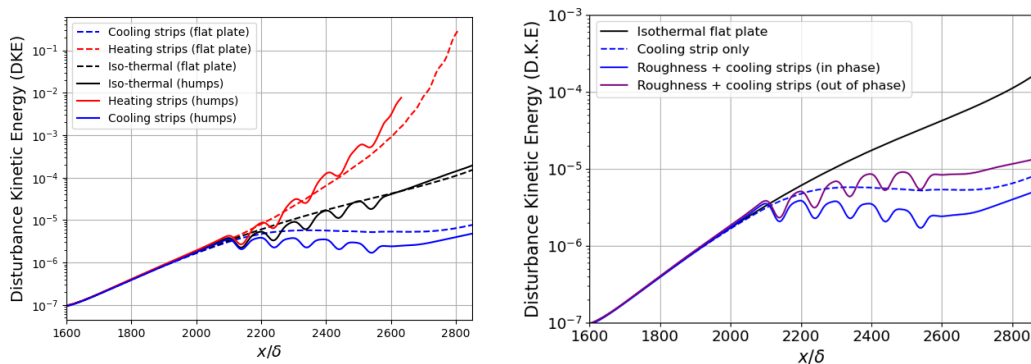

FIG. 8. Left: Disturbance kinetic energy along the streamwise direction for the limit heating and cooling cases: $T_{\text{wall}}/T_{\infty} = 1.335$ and $T_{\text{wall}}/T_{\infty} = 0.665$. Right: Effect of the phase shift of the cooling strips. The roughness patch is located between $x/\delta = [2090, 2590]$.
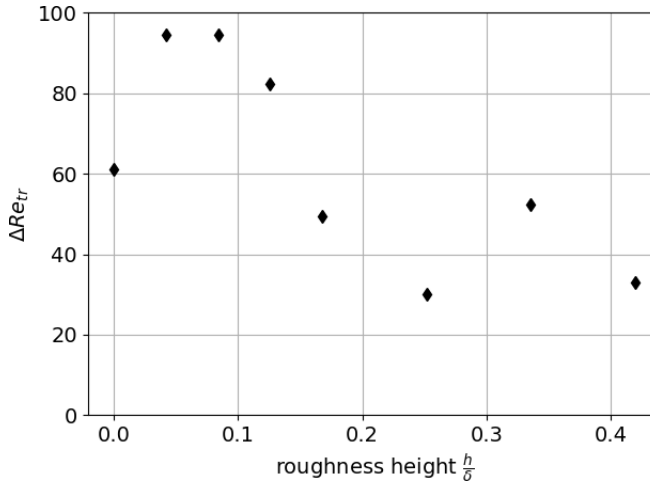
FIG. 9. Influence of the physical roughness height on the stability of the flow.

Fig. 5) and vary the height of the physical roughness element using the similarly defined $\Delta \mathrm{Re}_{tr}$. The small physical roughness acts to delay transition from a cooled wall alone; at sufficiently large physical roughness elements, the flow is destabilized by these perturbations as the physical roughness induces premature transition and overpowers any stabilization mechanism. In Fig. 8, due to the logarithmic scale, the stabilizing effect the combination of physical and thermodynamic (cooling) roughness appears modest. The contour plot of the DKE, shown in Fig. 10, offers a more fair comparison of the stabilization caused by the combined effects of cooling and roughness. Here, the color range is identical for all panels. As we can see, the cooling strips are very effective at reducing the amplitude of the disturbances in the near-wall region but are even more efficient at eliminating the onset of instabilities in the region above the boundary layer. The disturbances above the boundary layer are particularly destabilizing and usually accompanied by a rapid growth of secondary instabilities. The cases featuring cooling strips are extremely efficient at neutralizing these freestream instabilities, suggesting a stronger damping effect on the higher frequencies. To verify this assumption, the wall friction spectrum for different regions of the flow is shown in Fig. 11. The colors indicate the wall temperature; each line style represents a different portion of the wall, which is identified in the caption. Starting with the effect of the heating strips alone, we first observe in Fig. 11 (left) that the heating strips tend to amplify the whole frequency spectrum, but more specifically, the off-peak frequencies as we observe a broader peak around the dominant frequency. This effect is even more noticeable at the $2F$ harmonic for which the neighboring frequencies experience considerably higher amplification, which leads to the formation of a local minimum near $F \approx 32$. The cooling strips induce the opposite effect; we observe a dampening effect on the off-peak frequencies, which makes the dominant frequency more easily distinguishable. However, this time, we see the emergence of a peak near $F \approx 32$ and 45. Recalling that the dominant inlet TS frequency is $F = 18$, and its harmonics are $F = 36, 54, 72$, etc. It is interesting to note that, in the presence of cooling strips, we observe the formation of two other peaks at frequencies ($F = 32, 45$) that are not multiples of the fundamental TS frequency ($F = 18$) nor of the cooling strips ($F = 39$). This effect is more pronounced in the presence of roughness as seen in Fig. 11 (right), but the frequencies remain the same, leading us to believe that the periodic excitation of the flow, whether by the use of temperature strips or smooth wall roughness, induces the formation of off-harmonic perturbations. The use of a finite-bandwidth approach was crucial to this observation as in a classical discrete representation, only the dominant mode and its harmonics would be solved ($F, 2F, 3F, \ldots$).
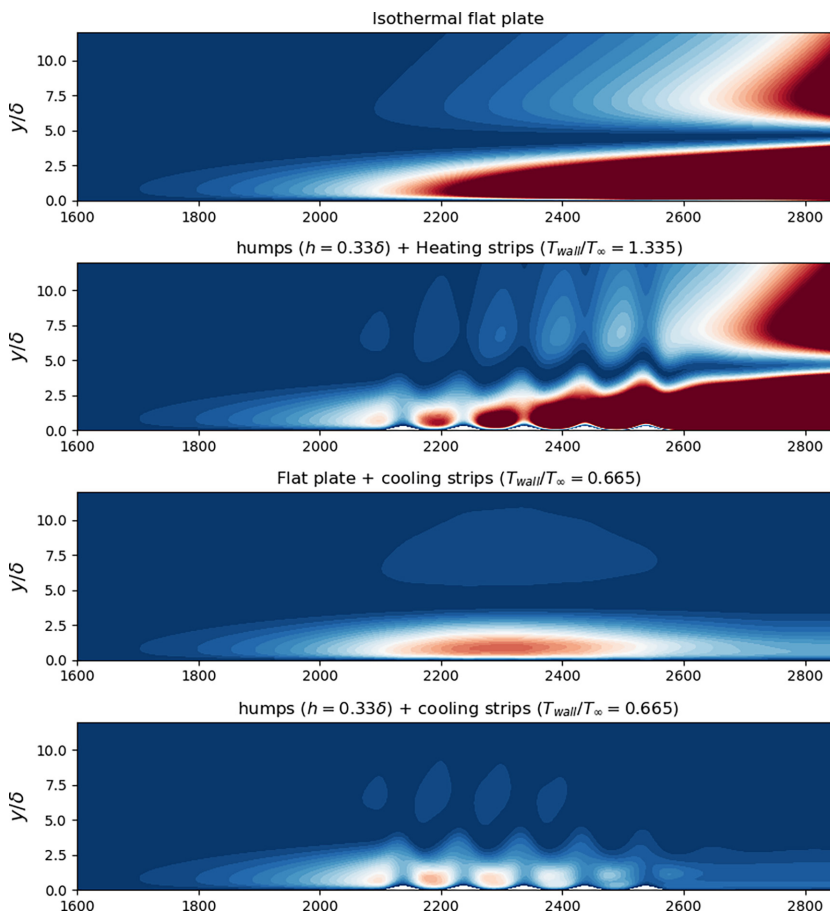
FIG. 10. Contour plot of the DKE. The color range from blue (DKE $= 0$) to red (DKE $= 4 \times 10^{-6}$) and is the same for all plots. The roughness patch is located between $x/\delta = [2090, 2590]$.
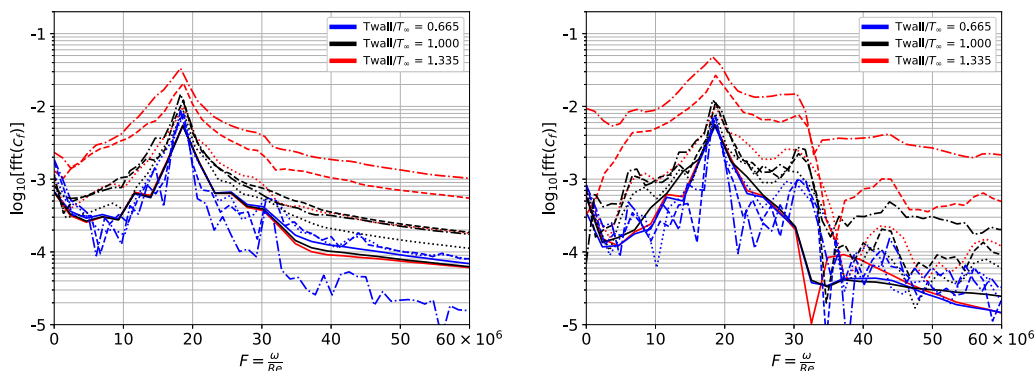

FIG. 11. fft (c_f) for different wall regions with only thermodynamic roughness (left) and a combination of physical and thermodynamic roughness (right). Each line style corresponds to a different region (—— is $x \in [1600, 2140]$, ········ is $x \in [1600, 2340]$, $----$ is $x \in [1600, 2540]$, and $-\cdot-\cdot-\cdot-$ is $x \in [1600, 2640]$).

IV. CONCLUSION

The coupling effect between physical and thermodynamic roughnesses on a flat-plate boundary layer is investigated under near-transonic conditions using the NPSE. To this end, we first study the effect of heating and cooling strips on the stability of a zero-pressure gradient flat-plate boundary layer. The sinusoidal cooling strip stabilizes the boundary layer and can delay the location of the transition to turbulence. Thereafter, the combined effect of physical and thermodynamic roughnesses is investigated using five sinusoidal two-dimensional humps, which were in phase with the sinusoidally varying thermodynamic roughness. The thermal strips and the roughness elements are located after the onset of instability (branch I) and extend over a range of 500δ. Both the heating strips and the roughness patch are defined using the same mathematical expression. The NPSE-based parametric study confirms the stabilizing effect of cooling strips and the destabilizing effect of heating strips on the stability of TS waves in the ZPG flat-plate scenario. The quantitative analysis reveals a spectral broadening in the presence of heating and a spectral narrowing in the presence of cooling. The NPSE study revealed a catalytic coupling effect between the temperature strips and the roughness. In other words, compared to the flat-plate case, the stability of the flow decreases in the presence of heating strips and roughness. Inversely, in comparison to the flat-plate case, the stability increases in the presence of cooling strips and roughness as long as the cooling and physical roughness are in phase, and the roughness element height is small enough to not induce a precocious transition. Whereas the physical roughness is inherently destabilizing to the boundary layer, the combination of in-phase sinusoidally varying wall cooling can result in a stabilization and delayed transition. The addition of cooling strips to wall roughness stabilizes the flow by acting on three fronts: Dampen the dominant instability modes in the flow, reduce the inflectional instability by locally decreasing the viscosity (thus, modifying the velocity profile), and induce a downward velocity by increasing the local density. These observations can be used to further stabilize boundary layer flows in aerospace applications where wall roughness cannot be avoided.

[1] J. Driver and D. Zingg, Optimized natural-laminar-flow airfoils, in *44th AIAA Aerospace Sciences Meeting and Exhibit* (AIAA, Reno, NV, 2006), pp. 1–16.

[2] Z.-H. Han, J. Chen, K.-S. Zhang, Z.-M. Xu, Z. Zhu, and W.-P. Song, Aerodynamic shape optimization of natural-laminar-flow wing using surrogate-based approach, AIAA J. **56**, 2579 (2018).

[3] R. L. Campbell and M. N. Lynde, Building a practical natural laminar flow design capability, in *35th AIAA Applied Aerodynamics Conference* (AIAA, Denver, CO, 2017), pp. 1–21.

[4] A. Kurz, S. Grundmann, C. Tropea, M. Forte, A. Seraudie, O. Vermeersch, D. Arnal, R. Goldin, and R. King, Boundary layer transition control using DBD plasma actuators, Aerospace Lab. **6**, 1 (2013).

[5] J. A. Masad and A. H. Nayfeh, Laminar flow control of subsonic boundary layers by suction and heat-transfer strips, Phys. Fluids A **4**, 1259 (1992).

[6] J. H. M. Fransson and P. H. Alfredsson, On the hydrodynamic stability of channel flow with cross flow, Phys. Fluids **15**, 436 (2003).

[7] F. E. Fish, P. W. Weber, M. M. Murray, and L. E. Howle, The tubercles on humpback whales' flippers: Application of bio-inspired technology, Integr. Comp. Biol. **51**, 203 (2011).

[8] A. V. Boiko, V. V. Kozlov, V. V. Syzrantsev, and V. A. Shcherbakov, Riblet control of the laminar-turbulent transition in a stationary vortex on an oblique airfoil, J. Appl. Mech. Tech. Phys. **37**, 69 (1996).

[9] J. Zahn and U. Rist, Impact of deep gaps on laminar - Turbulent transition in compressible boundary-layer flow, AIAA J. **54**, 66 (2016).

[10] J. H. M. Fransson, A. Talamelli, L. Brandt, and C. Cossu, Delaying Transition to Turbulence by a Passive Mechanism, Phys. Rev. Lett. **96**, 064501 (2006).

[11] J.-C. Loiseau, J.-C. Robinet, S. Cherubini, and E. Leriche, Investigation of the roughness-induced transition: Global stability analyses and direct numerical simulations, J. Fluid Mech. **760**, 175 (2014).

[12] M. A. Bucci, D. K. Puckert, C. Andriano, J.-C. Loiseau, S. Cherubini, J.-C. Robinet, and U. Rist, Roughness-induced transition by quasi-resonance of a varicose global mode, J. Fluid Mech. **836**, 167 (2018).

[13] L. Siconolfi, S. Camarri, and J. H. M. Fransson, Stability analysis of boundary layers controlled by miniature vortex generators, J. Fluid Mech. **784**, 596 (2015).

[14] P. Balakrishnan and K. Srinivasan, Jet noise reduction using co-axial swirl flow with curved vanes, Applied Acoustics **126**, 149 (2017).

[15] J.-P. Hickey, K. Younes, M. X. Yao, D. Fan, and J. Mouallem, Targeted turbulent structure control in wall-bounded flows via localized heating, Phys. Fluids **32**, 035104 (2020).

[16] T. Bon and J. Meyers, Stable channel flow with spanwise heterogeneous surface temperature, J. Fluid Mech. **933**, A57 (2022).

[17] J. Pralits and A. Hanifi, Optimization of steady suction for disturbance control on infinite swept wings, Phys. Fluids **15**, 2756 (2003).

[18] A. V. Dovgal, V. Y. Levchenko, and V. A. Timopeev, Boundary layer control by a local heating of the wall, in *Laminar-Turbulent Transition*, edited by D. Arnal and R. Michel (Springer, Berlin/Heidelberg, 1990), pp. 113–121.

[19] H. W. Liepmann, G. L. Brown, and D. M. Nosenchuck, Control of laminar-instability waves using a new technique, J. Fluid Mech. **118**, 187 (1982).

[20] D. M. Bushnell, Aircraft drag reduction—a review, J. Aerosp. Eng. **217**, 1 (2003).

[21] J. A. Masad and R. Abid, On transition in supersonic and hypersonic boundary layers, Int. J. Eng. Sci. **33**, 1893 (1995).

[22] J. Pralits, Optimal design of natural and hybrid laminar flow control on wings, Ph.D. thesis, KTH, Stockholm, 2003.

[23] X. Liang, X. Li, D. Fu, and Y. Ma, Effects of wall temperature on boundary layer stability over a blunt cone at Mach 7.99, Comput. Fluids **39**, 359 (2010).

[24] V. Soudakov, A. Fedorov, and I. Egorov, Stability of high-speed boundary layer on a sharp cone with localized wall heating or cooling, Progress in Flight Physics **7**, 569 (2015).

[25] A. Fedorov, V. Soudakov, I. Egorov, A. Sidorenko, Y. Gromyko, D. Bountin, P. Polivanov, and A. Maslov, High-speed boundary-layer stability on a cone with localized wall heating or cooling, AIAA J. **53**, 2512 (2015).

[26] F. Oz, T. E. Goebel, J. S. Jewell, and K. Kara, Local wall cooling effects on hypersonic boundary-layer stability, J. Spacecr. Rockets **60**, 412 (2023).

[27] R. Zhao, C. Wen, X. Tian, T. Long, and W. Yuan, Numerical simulation of local wall heating and cooling effect on the stability of a hypersonic boundary layer, Int. J. Heat Mass Transf. **121**, 986 (2018).

[28] J. A. Masad and V. Iyer, Transition prediction and control in subsonic flow over a hump, Phys. Fluids **6**, 313 (1994).

[29] A. Al-Maaitah, A. Nayfeh, and S. Ragab, Effect of wall cooling on the stability of compressible subsonic flows over smooth humps and backward-facing steps, Phys. Fluids A **2**, 381 (1990).

[30] F. Lacombe and J.-P. Hickey, Krypton: Nonlinear parabolized stability equation solver for transonic flow in curvilinear coordinates, SoftwareX **20**, 101206 (2022).

[31] A. A. Khan, T. Liang, A. Batista, and J. Kuehl, On energy redistribution for the nonlinear parabolized stability equations method, Fluids **7**, 264 (2022).

[32] F. Lacombe and J.-P. Hickey, The role of two-dimensional roughness on the modal instability in compressible boundary layers (unpublished).

[33] F. Lacombe, Stability of compressible boundary layers in presence of smooth roughness and wall temperature effects, Ph.D. thesis, University of Waterloo, 2023.

[34] M. Dong and A. Zhang, Scattering of Tollmien-Schlichting waves as they pass over forward-/backward-facing steps, Appl. Math. Mech. **39**, 1411 (2018).